Acta Pharmaceutica Sinica B 2020;10(10):1954−1965

Chinese Pharmaceutical Association
Institute of Materia Medica, Chinese Academy of Medical Sciences

Acta Pharmaceutica Sinica B

www.elsevier.com/locate/apsb
www.sciencedirect.com

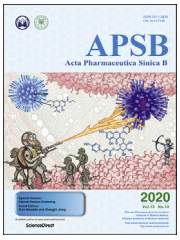

ORIGINAL ARTICLE

Structure, property, biogenesis, and activity of diterpenoid alkaloids containing a sulfonic acid group from *Aconitum carmichaelii*

Qinglan Guo[†], Huan Xia[†], Yuzhuo Wu, Shuai Shao, Chengbo Xu, Tiantai Zhang[*], Jiangong Shi[*]

State Key Laboratory of Bioactive Substance and Function of Natural Medicines, Institute of Materia Medica, Chinese Academy of Medical Sciences and Peking Union Medical College, Beijing 100050, China

Received 24 October 2019; received in revised form 18 December 2019; accepted 17 January 2020

KEY WORDS

Ranunculaceae;
Aconitum carmichaelii;
Sulfonated C_{20}-diterpenoid alkaloid;
Aconicarmisulfonines;
Chuanfusulfonine A;
Analgesic effect

Abstract Three new C_{20}-diterpenoid alkaloids with a sulfonic acid unit, named aconicarmisulfonines B and C (**1** and **2**) and chuanfusulfonine A (**3**), respectively, were isolated from the *Aconitum carmichaelii* lateral roots ("fu zi" in Chinese). Structures of **1**−**3** were determined by spectroscopic data analysis. Intriguing chemical properties and reactions were observed for the C_{20}-diterpenoid alkaloids: (a) specific selective nucleophilic addition of the carbonyl (C-12) in **1** with CD_3OD; (b) interconversion between **1** and **2** in D_2O; (c) stereo- and/or regioselective deuterations of H-11α in **1**−**3** and both H-11α and H-11β in aconicarmisulfonine A (**4**); (d) TMSP-2,2,3,3-d_4 promoted cleavage of the C-12−C-13 bond of **4** in D_2O; (e) dehydrogenation of **4** in pyridine-d_5, and (f) Na_2SO_3-assisted dehydrogenation and *N*-deethylation of songorine (**5**, a putative precursor of **1**−**4**). Biogenetically, **1** and **2** are correlated with **4**, for which the same novel carbon skeleton is proposed to be derived from semipinacol rearrangements *via* migrations of C-13−C-16 and C-15−C-16 bonds of the napelline-type skeleton, respectively. Meanwhile, **3** is a highly possible precursor or a concurrent product in the biosynthetic pathways of **1**, **2**, and **4**. In the acetic acid-induced mice writhing assay, at 1.0 mg/kg (i.p.), compounds **1**, **2**, **5**, **5a**, and **5b** exhibited analgesic effects against mice writhing.

*Corresponding authors. Tel.: +86 10 63025166; fax: +86 10 63017757.
E-mail addresses: ttzhang@imm.ac.cn (Tiantai Zhang), shijg@imm.ac.cn (Jiangong Shi).
[†]These authors made equal contributions to this work.
Peer review under responsibility of Chinese Pharmaceutical Association and Institute of Materia Medica, Chinese Academy of Medical Sciences.

https://doi.org/10.1016/j.apsb.2020.01.013

1. Introduction

C_{20}-Diterpenoid alkaloids are a group of natural products with distinctive diverse carbon skeletons[1,2]. Approximate 400 members have been reported and divided into four classes including at least 24 types, 34 subtypes, and 42 groups[1–5]. Plants of two genera *Aconitum* and *Delphinium* in the Ranunculaceae family and of one genus *Spiraea* in the Rosaceae family are the richest source of the C_{20}-diterpenoid alkaloids[1,2]. Due to variable chemical properties, notable pharmacological profiles, and structurally sophisticated architectures, considerable interest from the community of medicinal and organic chemistry has been elicited over 130 years[1,2,6], leading to recent fruitful achievements in total synthesis of a subset of C_{20}-diterpenoid alkaloids[7–12]. The dried lateral root ("fu zi" in Chinese) of the poisonous plant *Aconitum carmichaelii* Debx. is an important ingredient of many preparations and formulations for the treatment of various pains in the oriental countries[13–15]. To reduce fatal poisoning, "fu zi" is cautiously utilized by processing, decocting, or formulating[16–19]. Previous studies chemically and pharmacologically revealed aconitine-type C_{19}-diterpenoid alkaloids representing the predominant toxic and active constituents of this herbal medicine[20], while a majority of toxic C_{19}-diterpenoid alkaloid diesters were hydrolyzed into less toxic monoester and/or alcohol forms during processing and decocting[21–23]. Nevertheless, the currently known chemical constituents were mostly separated from organic solvent extracts of the drug materials. Meanwhile, HCl and/or NH_4OH were used in extraction and/or isolation steps[3–5,14,15,24–30]. Particularly the extraction methods differ from that classically decocts "fu zi" with water. Thus, as part of a program to detailly search for water-soluble active constituents from several popular traditional Chinese medicines and to test their pharmacological effects[31–38], we focused on an aqueous extract of the air-dried raw material of "fu zi", which is closer to a practically prepared decoction. From the extract, 54 previously unknown constituents have been reported, including 12 unprecedented glycosidic C_{19}-diterpenoid alkaloids and three sulfonated C_{20}-diterpenoid alkaloids with two novel carbon architectures, as well as their notable analgesic effects[39–47]. Further examination of a remaining fraction of the extract has resulted in characterization of three additional sulfonated C_{20}-diterpenoid alkaloids (**1**–**3**, Fig. 1). Herein, we report details of their isolation, structural elucidation, distinctive chemical properties, plausible biogenesis, and analgesic effects.

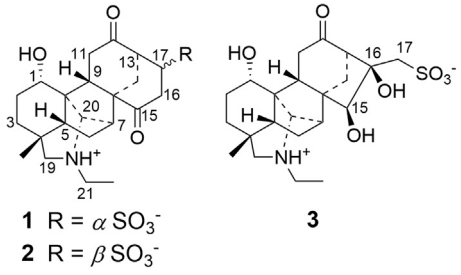

Figure 1 Structures of compounds **1**–**3**.

2. Results and discussion

2.1. Structure elucidation of *1*–*3*

Compound **1** was obtained as a white amorphous powder with $[\alpha]_D^{20}$ −38.1 (*c* 0.29, MeOH). The presence of hydroxyl and/or amino (3393 cm^{-1}) and ketone carbonyl (1738 and 1678 cm^{-1}) units in its molecule was deduced from the characteristic absorption bands in the IR spectrum of **1**. Hydrogen adduct ion peaks of the molecule at *m/z* 438 $[M+H]^+$ and 436 $[M-H]^-$ were detectable by positive and negative modes of ESI-MS, respectively. Subsequent measurements of HR-ESI-MS data (see Experimental Section) determined the molecular formula as $C_{22}H_{31}NO_6S$. Diagnostic signals for a C_{20}-diterpenoid alkaloid[40,42,43,45,47] were exhibited in the ^1H NMR spectrum of **1** in D_2O, including two heteroatom-bearing methines at δ_H 4.12 (brdd, J = 9.0 and 8.4 Hz, H-1) and 4.00 (brs, H-20), a methyl group at δ_H 0.91 (s, H_3-18), and a characteristic *N*-ethyl unit at δ_H 3.32 (m, H_2-21) and 1.38 (t, J = 7.2 Hz, H-22), in addition to five aliphatic methines and seven aliphatic methylenes between δ_H 3.61 and 1.46 (partially overlapping multiplets). Corresponding to the abovementioned structural units, 22 carbon resonances including two carbonyl carbons at δ_C 217.0 (C-12) and 216.3 (C-15) as well as three additional sp^3 hybrid quaternary carbons at δ_C 35.2 (C-4), 53.5 (C-8), and 52.6 (C-10) (Table 1) were observable in the ^{13}C NMR and DEPT spectra of **1**. These spectroscopic data were similar to those reported for aconicarmisulfonine A (**4**, Scheme 1) from the same extract[45]. Analyzing the 2D NMR spectroscopic data of **1**, the same rare skeletal architecture and 1-hydroxy-12-one substitution pattern sharing by the two compounds were readily determined. However, a 15-ketone in **1** replacing the 16-one in **4** was revealed by the long-range heteronuclear correlation signals of C-15/H-9, H_2-14, H_2-16, and H-17 in the HMBC spectrum and the homonuclear vicinal coupling correlation peaks of H-16b/H-17/H-13 in the $^1H-^1H$ COSY spectrum (Fig. 2). A 17-sulfonate in **1** was assigned to satisfy the molecular formula and substitution of C-17, and its α-orientation was elucidated from the NOE cross-peak between H-9 and H-17 in the ROESY spectrum (Fig. 3), wherein the remaining NOE correlation signals proved identity of the relative configuration of other chiral centers in **1** and **4**. Based on biogenetic consideration of the identical carbon skeleton deriving from the same precursor (Scheme 2), stereochemistry of **1** and **4** was predicted to be the same except for an additional 17*R*-configuration in **1**, of which **4** was verified by a single crystal X-ray diffraction[45]. Further supportive evidences for the prediction were obtained from explanation of a negative Cotton effect at 290 ($\Delta\varepsilon$ −0.43) nm arising from $n-\pi^*$ transitions of the carbonyl chromophores in the CD spectrum (Supporting Information Fig. S11) by the octant rule for the cyclohexanones[48,49] as well as the consistency between the measured CD and theoretically calculated ECD spectra of **1**. Thus, compound **1** was determined to have the structure analogized to aconicarmisulfonine A and named aconicarmisulfonine B.

Compound **2**, a white amorphous powder with $[\alpha]_D^{20}$ −37.4 (*c* 0.14, MeOH), had spectroscopic data very similar to those of **1**. However, comparing the NMR spectroscopic data of the two compounds in the same solvent D_2O (Table 1), coupling constant and chemical shift changes of H-13 and H-17 from the broad singlet (δ_H 3.27, $J_{13,16}$ ~0 Hz) and broad doublet (δ_H 2.74,

$J_{16,17b}$ = 10.2 Hz) in **1** into a doublet (δ_H 3.29, $J_{13,16}$ = 8.4 Hz) and a double doublet (δ_H 3.11, $J_{13,16}$ = 8.4 Hz and $J_{16,17b}$ = 9.0 Hz) in **2** were distinguishable. In addition, upfield shifts by $\Delta\delta_C$ −1.0, −1.5, and −2.3 were observed for C-6, C-8, and C-16 in **2**, respectively, whereas downfield shifts by $\Delta\delta_C$ +1.2, +2.4, +1.1, +1.8, and +3.1 were observed for C-7, C-9, C-11, C-14, and C-17. From these data, **2** was deduced to be an epimer of **1** having a β-orientation of 17-sulfonate. The deduction was verified by 2D NMR spectroscopic data analysis (Figs. 2 and 3), especially by the NOE correlation signals between H-14a with H-11a and H-20 as well as between H-14b and H-17 (Fig. 3) in the ROESY spectrum of **2**. Based on similarity of the CD spectra between **1** and **2** as well as the consistency between the measured CD and calculated ECD spectra of **2**, the configurational change at C-17 does not affect significantly on the measured CD and calculated ECD spectra of the two compounds (Fig. 4). Therefore, compound **2** was determined as the 17-epimer of **1** and named aconicarmisulfonine C.

Compound **3**, a white amorphous powder with $[\alpha]_D^{20}$ −7.3 (*c* 0.15, MeOH), is another C_{20}-diterpenoid alkaloid having the molecular formula $C_{22}H_{33}NO_7S$ as deduced from HR-ESI-MS and NMR spectroscopic data. This compound displayed the NMR spectroscopic data (Table 1) similar to those of chuanfunine (previously isolated from the same plant)[50]. However, significant upfield shifts of H-15 and H_2-17 ($\Delta\delta_H$>−0.23) as well as C-15, C-16, and C-17 ($\Delta\delta_C$>−3.6) in **3** were shown when compared with that reported for chuanfunine[50]. From the differences of the NMR spectroscopic data and molecular formulae between the two compounds, **3** was elucidated to be a derivative of chuanfunine with substitution of 17-OH by 17-SO_3^-. The elucidation was decisively evidenced by the 2D NMR experimental data of **3**. Especially, the long-range correlation signals H_2-14/C-7, C-9, C-12, C-15, and C-16; H-15/C-7, C-9, C-13, C-16, and C-17; and H_2-17/C-13, C-15, and C-16 (Fig. 2) in the HMBC spectrum verified the napelline-type skeletal structure sharing by **3** and chuanfunine. Additionally, the NOE correlation signals H-7/H-14b, H-15, H-20, H_2-21, and H_3-22; H-14a/H-20; H-14b/H-15; and H-15/H_2-17 (Fig. 3) in the NOESY spectrum of **3** proved the β-orientation of 15-OH and 16-OH. A good similarity between the measured CD and calculated ECD spectra of **3** (Fig. 4) was supportive for the absolute configurational assignment. Hence, compound **3** was determined to be 17-dehydroxy-chuanfunine-17-sulfonic acid and designated as chuanfusulfonine A.

2.2. *Chemical properties of **1**–**4***

During measurements of the NMR spectra, distinctive stability in D_2O or CD_3OD was observable for **1** and **2**, respectively. Compound **2** was partially converted into **1** in D_2O accompanying by deuteration of H-11a (Fig. 5a and b), whereas **1** was partially transformed into a new product **1a** in CD_3OD (Fig. 6a and b). After storage in a refrigerator at 4 °C around 14 months, the

Table 1 The NMR spectroscopic data (δ) for compounds **1**–**3** in D_2O[a].

No.	**1**		**2**		**3**	
	δ_H	δ_C	δ_H	δ_C	δ_H	δ_C
1	4.12 brdd (9.0, 8.4)	67.3	4.08 brt (9.0)	67.3	4.12 dd (9.6, 8.4)	68.0
2a	2.14 m	30.9	2.11 m	30.9	2.13 m	31.0
2b	1.57 m		1.56 m		1.53 m	
3a	1.68 brd (13.8)	35.5	1.68 m	35.6	1.67 m	35.5
3b	1.46 dt (3.6, 13.8)		1.45 dt (3.0, 13.8)		1.47 brt (13.8)	
4		35.2		35.2		35.6
5	1.72 brd (7.8)	47.3	1.73 brd (7.8)	47.6	1.72 d (8.4)	47.1
6a	2.91 dd (15.0, 7.8)	22.1	3.31 dd (15.0, 7.8)	21.1	2.83 dd (14.4, 8.4)	22.4
6b	1.77 dd (15.0, 4.8)		1.66 dd (15.0, 4.8)		1.61 dd (14.4, 4.2)	
7	2.85 d (4.8)	40.8	2.98 d (4.8)	42.0	2.72 brd (4.2)	44.2
8		53.5		52.0		49.2
9	2.19 dd (11.4, 7.2)	42.9	2.03 dd (11.4, 7.2)	45.3	2.20 dd (10.2, 7.2)	36.6
10		52.6		52.8		52.6
11a	3.61 dd (16.8, 11.4)	37.9	3.52 dd (16.8, 11.4)	39.0	3.29 dd (12.0, 10.2)	38.1
11b	2.60 dd (16.8, 7.2)		2.49 dd (16.8, 7.2)		2.39 dd (12.0, 7.2)	
12		217.0		216.2		216.9
13	3.27 brs	47.4	3.29 d (8.4)	47.0	3.05 d (3.6)	56.2
14a	2.52 brd (13.2)	29.8	2.65 brd (12.6)	31.6	2.06 d (13.2)	29.5
14b	2.12 brd (13.2)		2.14 brd (12.6)		1.69 dd (13.2, 3.6)	
15		216.3		217.1	4.29 s	76.7
16a	3.23 brd (14.4)	50.8	3.11 brd (14.4)	48.5		76.5
16b	3.01 dd (14.4, 10.2)		2.83 dd (14.4, 9.0)			
17a	2.74 brd (10.2)	47.6	3.11 dd (9.0, 8.4)	50.7	3.26 d (14.4)	59.3
17b					3.20 d (14.4)	
18	0.91 s	24.5	0.91 s	24.5	0.91 s	24.7
19a	3.40 d (13.8)	57.2	3.39 d (13.2)	57.3	3.36 d (13.8)	57.7
19b	2.96 d (13.8)		2.97 d (13.2)		2.96 d (13.8)	
20	4.00 brs	65.1	4.03 brs	65.6	3.96 brs	65.4
21	3.32 m	54.9	3.32 m	54.9	3.30 q (7.2)	54.7
22	1.38 t (7.2)	10.1	1.39 t (6.6)	10.1	1.37 t (7.2)	10.1

[a]Chemical shift values (δ) were measured at 600 MHz for ^1H NMR and at 150 MHz for ^{13}C NMR, respectively. Proton coupling constants (*J*) in Hz are given in parentheses. The assignments were based on DEPT, ^1H–^1H COSY, HSQC, and HMBC experiments.

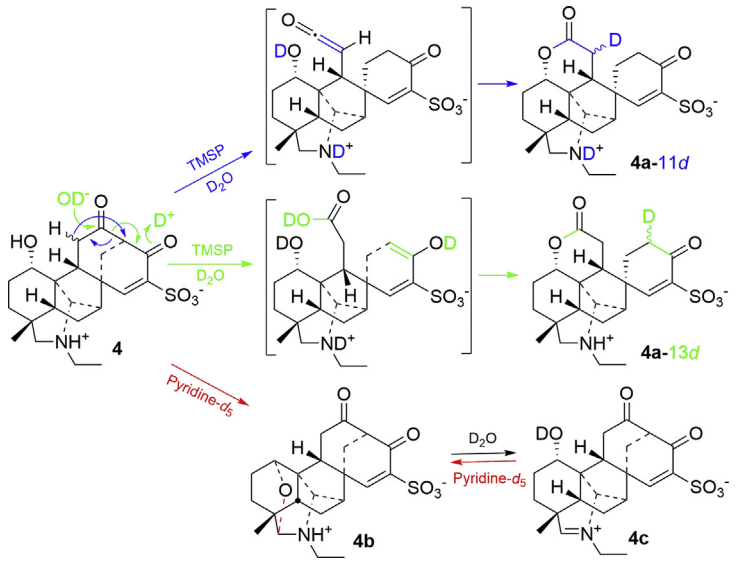

Scheme 1 Transformation from **4** to **4a** in D_2O containing TMSP-2,2,3,3-d_4 and to **4b** in pyridine-d_5.

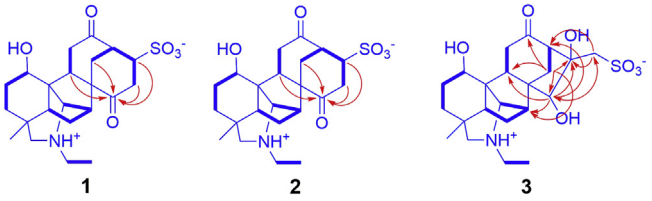

Figure 2 Main $^1H-^1H$ COSY (thick lines) and HMBC (arrows, from ^1H to ^{13}C) correlations of compounds **1**–**3** (Fig. S1).

samples of **1** and **2** in D_2O became almost identical, containing two components (**1**/**1-*d*** and **2-*d***) in an approximate 4:1 ratio (Fig. 5c–f). The gradual generation of **1a-*d*** from **1-*d*** was also demonstrated by measuring the ^1H NMR spectra of the mixture (Fig. 6c and d) as well as of a purified sample of **1-*d*** in CD_3OD (Fig. 7). The structures of **1-*d*** and **2-*d*** were readily deduced as the H-11a deuterated **1** and **2**, respectively, by comparing the NMR spectroscopic data (Supporting Information Tables S1 and S2) which were unambiguously assignable by analysis of the 2D NMR spectra of the mixture. Particularly disappearance of the H-11a signals and variation of the splitting patterns of H-9 and H-11b in the ^1H NMR spectra (Figs. 5 and 6) were the determinative proofs for the deduction. The α-orientation of H-11a was deducible from comparing the NMR spectroscopic data between **1-*d*** and **1** as well as between **2-*d*** and **2**, along with the NOE correlation H-1/H-11b in the ROESY spectrum of the mixture. The structures of **1a** and **1a-*d*** were elucidated to be the semi-acetals deriving from nucleophilic addition of the solvent CD_3OD to 12-ketone in **1** and **1-*d***, respectively. The elucidation was based on distinguishing the signals between **1a** and **1** as well as between **1a-*d*** and **1-*d*** (Table S1) in the NMR spectra of the mixtures, especially on a characteristic resonance for a dioxygen-bearing quaternary carbon (δ_C 104.0) of **1a-*d*** or **1a** replacing the carbonyl carbon resonance (C-12) of **1-*d*** (δ_C 213.6) or **1** (δ_C 213.9), in combination with the HMBC correlations of the dioxygen-bearing quaternary carbon with H-11b, H-13, and H-14a. After evaporation of the CD_3OD solutions, the signals of **1a** or **1a-*d*** completely disappeared in the NMR spectra of the samples in D_2O, whereas those of **1** and **1-*d*** were retained, indicating that **1a** and **1a-*d*** survived only in CD_3OD. Therefore, accompanying the selective deuteration of H-11α (H-11a), **1** and **2** are able to interconvert to reach an equilibration in the approximate 4:1 ratio in D_2O, wherein **1** is a stable species with the higher abundance while **2** is less stable and relatively easier to isomerize into **1** (Scheme 3). Whereas, the 12-ketone in **1** has a more active chemical character to be selectively attacked by a nucleophile (CD_3OD) to produce a returnable ketone

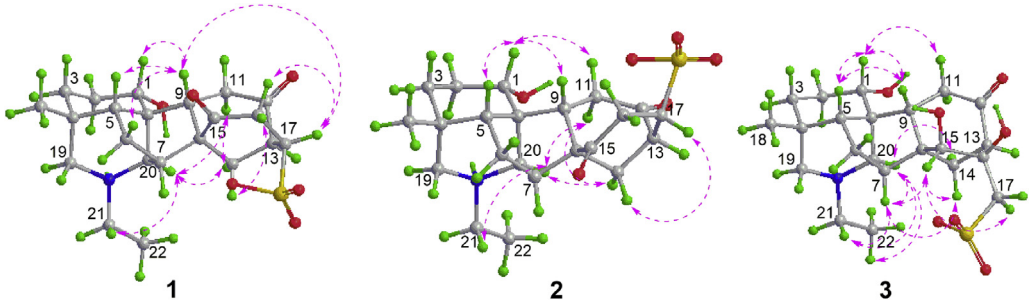

Figure 3 Main NOE correlations (pink dashed double arrows) of compounds **1**–**3**.

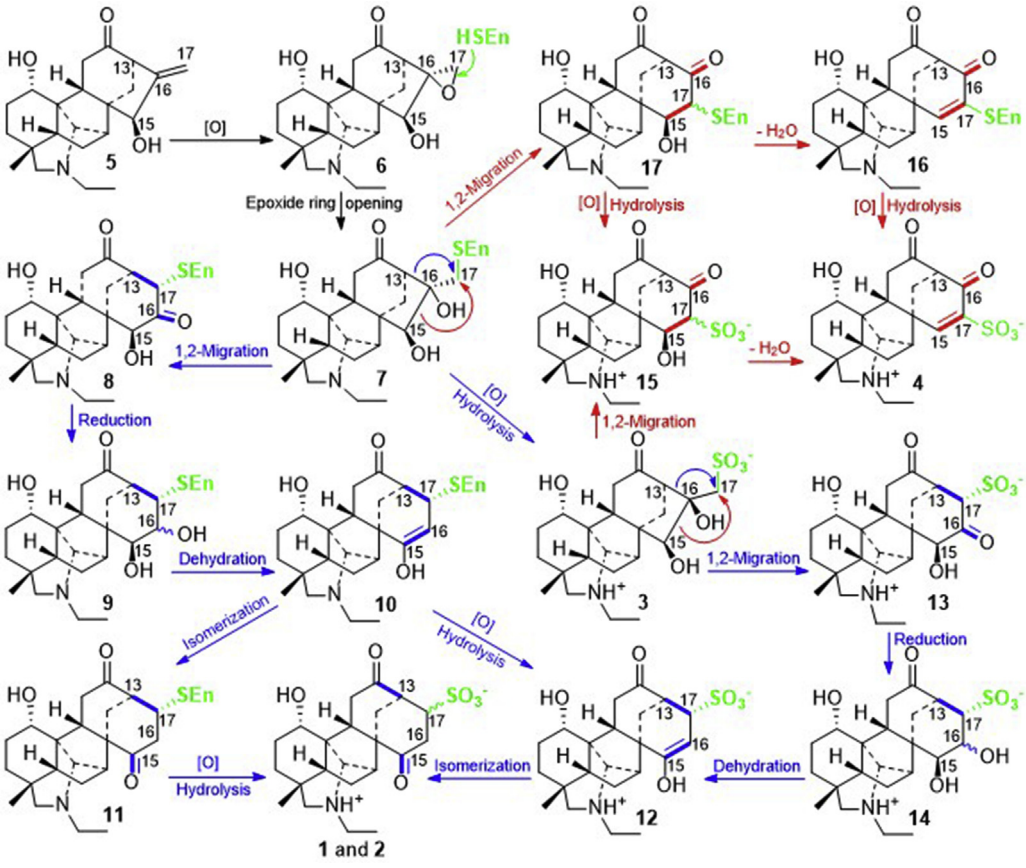

Scheme 2 Proposed biogenetic pathways for **1**−**4**.

semi-acetal. An explanation for the different properties between **1** and **2** is from the varied effects of the sulfonate group.

Differing from **1** and **2**, compound **3** was almost insoluble in CD_3OD. The selective deuteration of H-11α was also observed in the NMR spectra of **3** in D_2O. However, both H-11α and H-11β in **4** were readily deuterated in D_2O[45]. Because deuteration of the carbon-bearing protons was not observed in other diterpenoid alkaloids[42], the intriguing property of **1**−**4** must be due to the characteristic structural sulfonation. Particularly in the measurements of the NMR spectra of **4** in D_2O with and without using sodium 3-trimethylsilylpropionate (TMSP-2,2,3,3-d_4) as an internal reference, a product **4a** was gradually formed only in the solution containing TMSP. This suggested a TMSP promoted reaction of **4** to yield **4a**. HPLC separation of the sample afforded **4a** with recovering **4**. HR-ESI-MS indicated an isomeric relationship between **4a** and **4**. However, the NMR spectroscopic data of **4a** differed significantly from those of **4** (Supporting Information Table S3), showing replacement of the ketone carbonyl (C-12) and methine (CH-13) units in **4** by carboxylic carbon (δ_C 176.5) and methylene [δ_H 2.76 (dd, J = 13.2, 12.0 Hz) and 2.65 (brd, J = 12.0 Hz) and δ_C 35.3] in **4a**, respectively, along with the remarkable downfield shifts of H-1 and C-1. These spectroscopic data revealed a skeletal change from **4** to **4a**. The structure of **4a** was subsequently determined by analyzing the 2D NMR spectroscopic data. Briefly, a cleavage of the C-12−C-13 bond in **4** to give a 12-carboxyl in **4a** was deduced from the vicinal coupling cross-peaks H-9/H_2-11 and H_2-13/H_2-14 in the ^1H−^1H COSY spectrum as well as the long-range heteronuclear correlations H-1/C-2, C-9, and C-20; H-9/C-5, C-8, C-10, C-11, C-12, and C-14; H_2-11/C-8, C-9, C-10, and C-12; H_2-13/C-8, C-14, and C-16; H_2-14/C-8, C-15, and C-16; and H-15/C-8, C-9, C-14, C-16, and C-17 in the HMBC spectrum (Supporting Information Fig. S8). A lactone formation was constructed by the requirements of the molecular formula and chemical shift values of H-1 and C-1 and C-12. The NOE correlations between H-1 with H-9 and H-11a (Supporting Information Fig. S9) in the ROESY spectrum were supportive for the lactone and configuration of **4a**, though the expected correlation from H-1 to C-12 did not appear in the HMBC spectrum (possibly due to limitation of the sample amount). Hence, compound **4a** was assigned to have the structure deriving from an unprecedented intermolecular cleavage of the C-

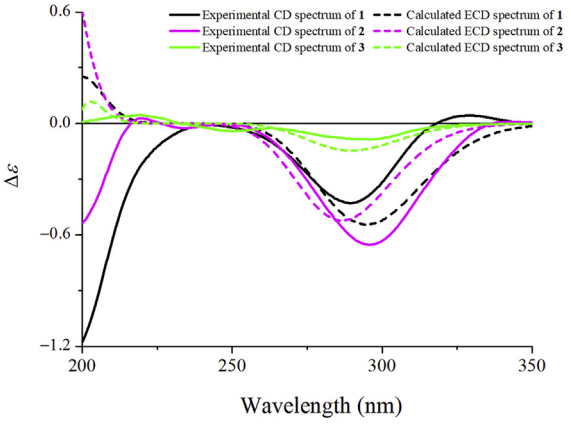

Figure 4 The overlaid experimental CD (full lines) and calculated ECD (dashed lines) spectra of **1**−**3**.

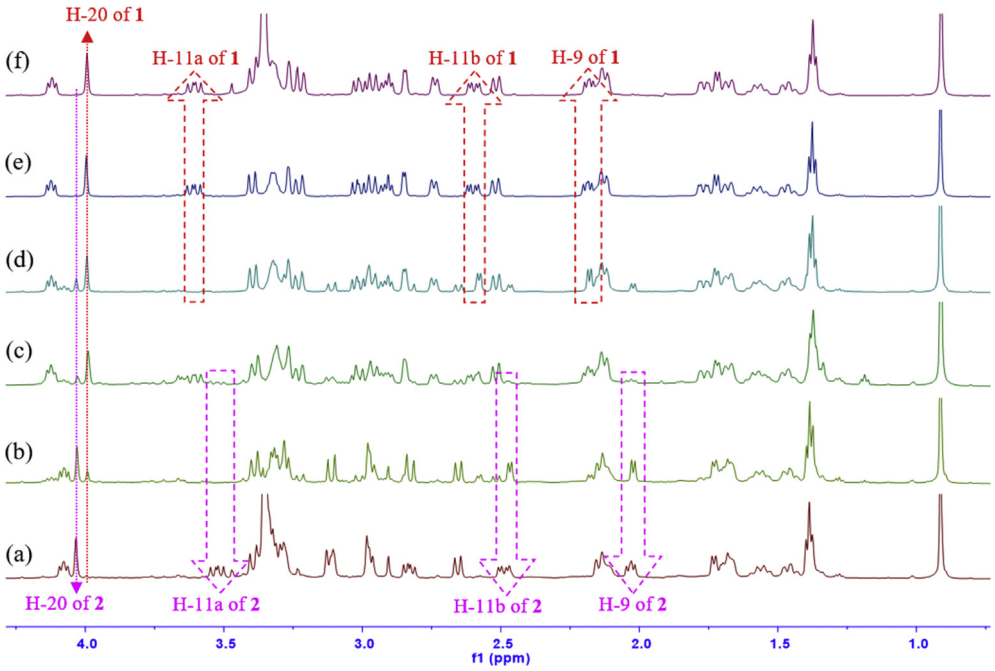

Figure 5 The overlaid ^{1}H NMR spectra of **2** (a)−(c) and **1** (d)−(f) in D_2O showing selective deuteration of H-11a and equilibration between **1-*d*** and **2-*d***. (a) initially obtained for **2**; (b) reacquired with the same sample of (a) after evaporated under reduced pressure to dry then re-dissolved in D_2O; (c) reacquired with the same sample of (b) after stored at 4 °C for 14 months (the splitting of H-9 and appearing of H-11a and H-11b may be explained by the presence of a relative larger amount of H_2O, which was partially introduced during storage of the sample, see the full spectra in Fig. S93−S95); (d) reacquired with the same sample of (e) after stored at 4 °C for 14 months; (e) reacquired with the same sample of (f) after evaporated under reduced pressure to dry and re-dissolved in D_2O; (f) initially obtained for **1**.

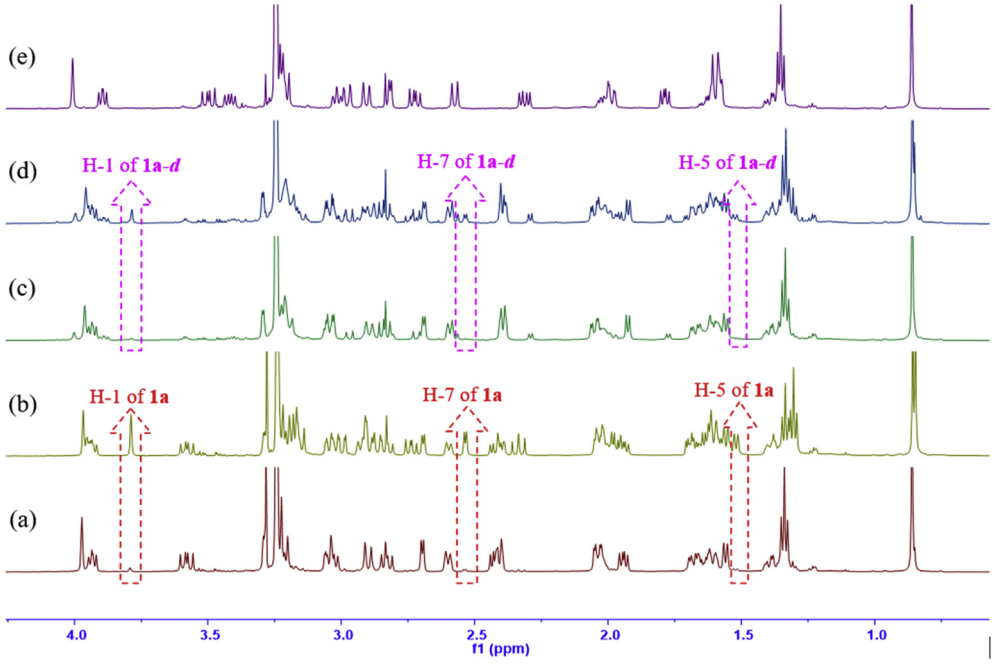

Figure 6 The overlaid ^{1}H NMR spectra of 1 in CD_3ODshowing production of **1a** or **1a-*d*** (a)−(d) and the ^{1}H NMR of **2** in CD_3OD showing no product formation (e). (a) initially obtained for **1**; (b) reacquired with the same sample of (a) after measurements of the ^{13}C NMR and DEPT spectra; (c) reacquired with the same sample of (b) after stored in D_2O at 4 °C for 14 months then evaporated under reduce pressure and re-dissolved in CD_3OD; (d) reobtained with the same sample of (c) after stored at 4 °C for two weeks; (e) initially obtained for **2** in CD_3OD.

12−C-13 bond in **4**. Although transformation mechanisms from **4** to **4a** could temporarily be proposed *via* a ketene intermediate with migration of one proton from C-11 to C-13 or a retro-Claisen reaction (Scheme 1), the two plausible mechanisms should result in deuteration of one proton at C-11 (*via* the ketene intermediate to give **4a**-11*d*) or C-13 (*via* the retro-Claisen reaction to give **4a**-13*d*). However, this was contrary to the observable H_2-11 and H_2-13 signals in the NMR spectra of **4a** (Supporting Information Fig. S108−S119). Therefore, the transformation mechanisms from **4** to **4a** seemed highly abnormal.

Because TMSP is a water-soluble salt with basicity, to inspect a possible promotion of the reaction by basicity (a suitable condition of the retro-Claisen reaction), **4** was treated with pyridine-d_5 in the NMR tube for a convenient detection of the reaction. After the pyridine-d_5 solution of **4** was stored at room temperature for 12 h, a new product **4b** was detectable by the NMR spectra. Analyzing the 1D and 2D NMR spectroscopic data of the reaction mixture (Supporting Information Table S3 and Figs. S8 and S9), **4b** was preliminarily elucidated to have an aza acetal structure deriving from dehydrogenation of **4**. Follow-up HPLC isolation of the reaction mixture afforded the product with recovering **4**. However, an iminium structure **4c** instead of the aza acetal **4b** was deducted from HR-ESI-MS as well as 1D and 2D NMR spectroscopic data of the product in D_2O (Table S3 and Figs. S8 and S9). Based on our previous investigation on transformation between the alcohol iminium and aza acetal forms of several C_{20}-diterpenoid alkaloids from the same extract[42], **4b** in pyridine-d_5 was speculated to be transformed into **4c** in D_2O (Scheme 1). The speculation was proved by the reacquired ^{1}H NMR spectrum of the sample in pyridine-d_5. Therefore, under the basic condition of pyridine-d_5, the C-12−C-13 bond in **4** was not cleaved to give **4a**, whereas **4b** was formed existing only as the alcohol iminium **4c** in D_2O. In addition, **4** was individually treated with equimolar sodium propionate (replacing TMSP) in H_2O or TMS in CD_3OD under room temperature for 48 h and then heating at 50 °C, TLC and HPLC analysis indicated that no product was produced in the solutions. Hence, TMSP must play an important role in transforming **4** into **4a**, which is unprecedented with currently unknown mechanism.

Additionally, in order to investigate possible artificial formation of **1**−**4**, the putative biosynthetic precursor songorine (**5**), obtained from the same extract in this study, was refluxed with sodium bisulfite (Na_2SO_3) in CH_3OH/H_2O (1:1) for 8 h. TLC and HPLC analysis of the reaction mixture showed production of two products **5a** and **5b** (Scheme 4). Following HPLC isolation of **5a** and **5b** from the reaction mixture, their structures were deduced from the HR-ESI-MS and NMR experimental data (Supporting Information Table S4 and Figs. S8 and S9) as deethylsongorine (**5a**)[51] and aconicarmichinium B (**5b**)[42], respectively. Although the former was isolated from *Aconitum monticola* in 1965 and recently studied by a single crystal X-ray diffraction, the full NMR spectroscopic data (Table S4) were absent in literature[51]. The later was previously obtained from the extract and proved to exist as the aza acetal and alcohol iminium forms in D_2O and pyridine-d_5[42], respectively. The Na_2SO_3-induced deethylation and dehydrogenation of diterpenoid alkaloids have never been reported. Furthermore, transformation from **3** to **1**, **2**, and/or **4** was not observed by refluxing **3** in water or HPLC mobile phase for 8 h. Therefore, artificial production of **1**−**4** from **5** as well as **1**, **2**, and/or **4** from **3** could preliminarily be excluded.

2.3. *Biogenetic relationships of **1**−**4***

According to the structural architectures of **1**−**3**, the co-occurring napeline-type C_{20}-diterpenoid alkaloid songorine (**5**)[45] is proposed to be their biosynthetic precursor (Scheme 2). The precursor undergoes sequentially enzyme-assisted double bond oxidation and epoxide ring opening through **6** to generate a key enzyme-adducting intermediate **7**. Semipinacol rearrangement[52] *via* 1,2-migration of the C-13−C-16 bond in **7** affords **8**. Subsequent

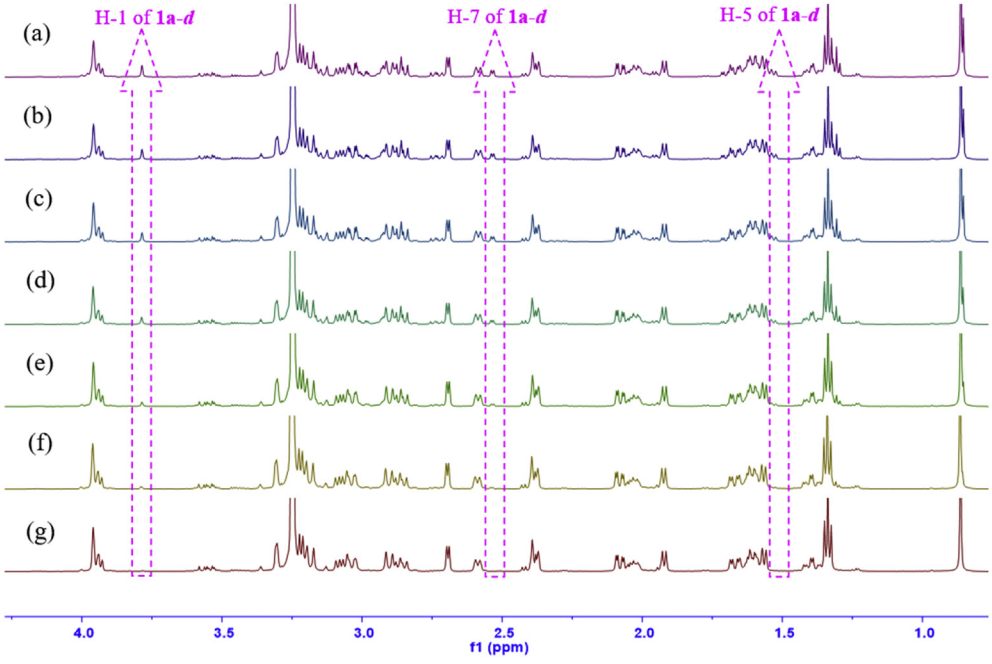

Figure 7 The overlaid ^{1}H NMR spectra of **1-*d*** in CD_3OD showing gradual formation **1a-*d***. (a)−(g) successively acquired with the same sample *via* a two-day interval.

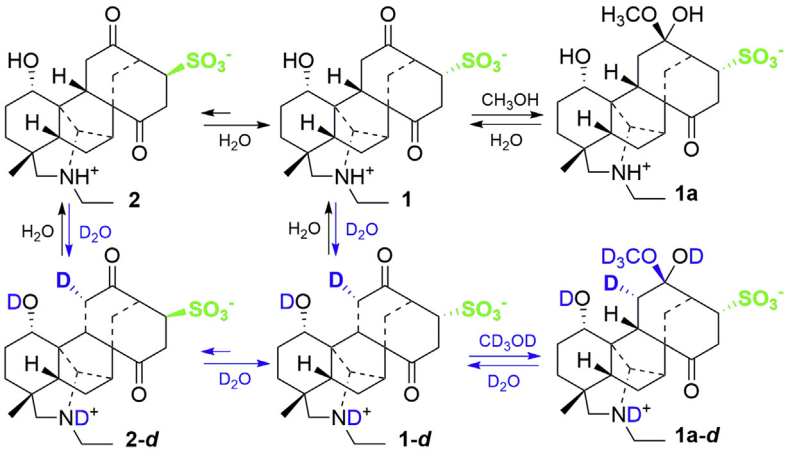

Scheme 3 Deuteration and conversion of **1** and **2** in D_2O and ketoacetal formation of **1** in CD_3OD.

enzyme-catalyzed selective hydrogenation of the newly formed carbonyl group in **8**, followed by concurrent or sequential dehydration *via* **9**, produces an enol intermediate **10**. The enol intermediate undergoes either oxidative hydrolysis and isomerization *via* **11** or a reverse sequence *via* **12** to afford **1** and/or **2**. Anyway, an equilibration between **1** and **2** would be achieved by interconversion in the aqueous biosystems since the equilibration was proved by the aforementioned experiments. Compound **3** is generated by oxidative hydrolysis of the intermediate **7**. As predicted in the biosynthetic pathway of **4** (red arrow part in Scheme 2)[45], **3** may be produced by a direct sulfonation of **5** and/or **6**. Alternatively, **1** and **2** would be generated *via* semipinacol rearrangement of the C-13−C-16 bond in **3**, followed by sequential or spontaneous reduction, dehydration, and isomerization through **13**, **14**, and **12**. Although **1** and **2** possess the same carbon skeleton as that of **4**[45], biogenetically **1** and **2** are proposed to be generated from the C-13−C-16 bond migration of the precursors while **4** from the C-15−C-16 bond migration. In particular, the coexistence of **1**−**4** in the extract not only supports the proposed biogenetic pathway (Scheme 2) but also indicates the biogenetic unselective migration of the C-13−C-16 and C-15−C-16 bonds in the key intermediates **7** or **3**. In order to keep the consistency with that of the precursor, the numbering for C-16 and C-17 in **4** is exchanged in **1** and **2**. In addition, the proposed biosynthetic pathways fully support assignment of the absolute configurations of **1**−**3** since the absolute configurations of **4**[45] and a derivative of **5**[42] were proved by single crystal X-ray diffraction.

2.4. *Analgesic activities of **1**−**3**, **4a**, **4c**, **5a**, and **5b***

Because "fu zi" is clinically used as an analgesic ingredient for the treatment of various pains and molecular targets of the unusual alkaloids are unpredictable, analgesic effects of the compounds on an available animal model of acetic acid-induced writhing assay[53] were preliminarily tested in this study (approved by the Animal Care & Welfare Committee Institute of Materia Medica, CAMS & PUMC). In spite of toxicity, flaconitine (3-acetylaconitine) was used as the positive control since it is a well identified analgesic constituent from the plants of the genus *Aconitum*. The assay result is given in Table 2 and Supporting Information Fig. S7. Comparing with the vehicle group, at 1.0 mg/kg (i.p.), compounds **1**, **2**, **5**, **5a**, and **5b** exhibited analgesic effects against mice writhing with inhibition rates >26%. Especially, at 1.0, 0.3, and 0.1 mg/kg (i.p.), dose-dependent inhibitions were exhibited by **5** and **5a**. Although the positive control gave a better inhibition (71.2%) at 0.3 mg/kg (i.p.), its toxicity was shown at 1.0 mg/kg (i.p.), however, toxicity was not observed for the other tested compounds. Due to interconversion between **1** and **2** is inevitable, their pharmacological effects must be contributed by equilibrations of the two compounds in the test samples. The two samples in this study were much less active than **4**[45], demonstrating that the absence of the conjugated ketene moiety in **1** and **2** significantly decreased the activity. In addition, ineffectiveness of **4a** and **4c** reveals that the carbon skeleton shared by **1**, **2**, and **4** was essential for the mice writhing inhibition. Comparison of the analgesic effects of **3**, **5**, **5a**, and **5b** sharing the napelline skeleton indicates that the exocyclic double bond is likely the most important pharmacophore since **3** was inactive, meanwhile, the activity was decreased by dislodging *N*-ethyl (**5a**) or leading-in iminium double bond (**5b**) in the structure.

3. Conclusions

Three sulfonated C_{20}-diterpenoid alkaloids (**1**−**3**) were discovered from *A. carmichaelii* lateral roots (fu zi). These compounds, along with aconicarmisulfonine A (**4**)[45] and aconicatisulfonines A and B[47] from the same extract, are the only sulfonated diterpenoid alkaloids from nature so far, architecturally covering three carbon skeletons. This unravels the general occurrence of sulfonation of the different types of diterpenoid alkaloids in this plant or the genus. Differential deuteration of H_2-11 in **1**−**4** in D_2O reveals that these compounds may actively interact with bioenvironments and biomolecules or targets to exhibit biological functions under physiological conditions. Chemical activity of H_2-11 in these compounds is highly peculiar since deuteration of H-13 locating between the two carbonyl groups (**1**, **2**, **4**, **4b**, and **4c**) or attaching to one carbonyl group (**3**, **4a**, **5**, **5a**, and **5b**) was not observable. Mutual transformation between **1** and **2** in D_2O indicates that the equilibration possibly exists in the aqueous biosystems to regulate their specific biological activities. Especially abundancy in the equilibration and selectivity of the nucleophilic addition show that **1** is more stable but chemically more active than **2**. These properties would play some roles in the pharmacological and biological functions of **1** and/or **2**. In addition, all the reactions, including the TMSP-2,2,3,3-d_4 promoted C-12−C-13 bond cleavage and dehydrogenation of **4** as well as the Na_2SO_3 assisted

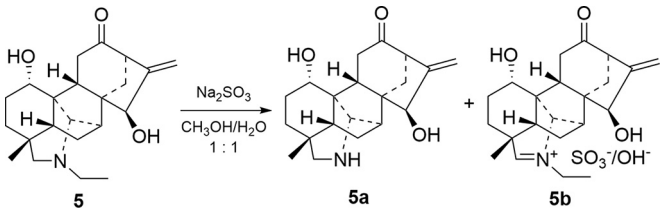

Scheme 4 Deethylation and dehydrogenation of **5**.

spontaneous dehydrogenation and deethylation of **5**, are unprecedented and useful for structural modification of the diterpenoid alkaloids under a relatively mild condition. The transformation from the aza acetal (**4b**) in pyridine-d_5 into alcohol iminium (**4c**) in D_2O is fully consistent with the behavior of several napelline-type diterpenoid alkaloids, indicating that the structural variation exists and possibly has biological/pharmacological significances under neutral, acidic, and alkali microenvironments of the biosystems[42]. Moreover, simultaneous isolation of **1**−**4** demonstrates a rational path for biogenetic and chemical synthesis of these C_{20}-diterpenoid alkaloids. Although **1** and **2** share the same carbon skeleton with **4**, the co-occurrence of **1**−**4** strongly supports the novel carbon skeleton deriving from the different carbon-bond migrations of the napelline-type precursor(s) *via* the semi-pinacol rearrangements in enzyme-involved biosynthesis. Especially **3** represents the most possible intermediate or the concurrent product in the biosynthetic pathway of **1**, **2**, and **4** though our attempts of chemical transformation from **3** to **1**, **2**, and **4** failed. Like amino acids having both the alkali (amine/iminium) and acidic (sulfonic acid) functionalities, the sulfonated diterpenoid alkaloids have specific zwitterionic properties and good biocompatibilities to play biological and/or pharmacological functions in the biosystems. The analgesic effects of the different types of C_{20}-diterpenoids testify that the multiple components work together in the clinic effects of this herbal medicine. The observed preliminary structure−activity relationships are helpful for new-drug development based on the C_{20}-diterpenoid leads. In summary, this study is opening a new window for the diterpenoid alkaloids in candidate discovery and new drug development as well as for the discovery of unknown functional molecules in the herbal medicine to support its clinic utilization. The protocols focusing on diverse constituents of the water extract, especially on minor components, should be validated for many of the Chinese herbal medicines.

4. Experimental

4.1. General experimental procedures

See Supporting Information.

4.2. Plant material

See Ref. 39.

4.3. Extraction and isolation

For preliminary extraction and isolation, see Refs. 39−46 and Supporting Information. Fraction C2-1-C-5 (13 g) was chromatographed over Sephadex LH-20 (H_2O) to yield C2-1-C-5-1−C2-1-C-5-6, of which C2-1-C-5-1 (0.8 g) was further fractionated by column chromatography (CC) over HW-40C, eluting with H_2O, to afford C2-1-C-5-1-1−C2-1-C-5-1-6. Purification of C2-1-C-5-1-4 (28 mg) by reversed phase HPLC (Ultimate XB-phenyl semi-preparative column, 20% CH_3OH in H_2O, containing 0.2% TFA, flow rate 2 mL/min) yielded **1** (5 mg, t_R = 56 min) and **2** (2 mg, t_R = 51 min). Fraction C2-1-C-5-4 (4 g) was separated by CC over Sephadex LH-20 (H_2O) to give C2-1-C-5-4-1−C2-1-C-5-4-7, of which C2-1-C-5-4-6 (1.1 g) was isolated by CC over reversed phase C-18 silica gel, eluted by a gradient mobile phase increasing MeOH (0 → 50%) in H_2O, to yield C2-1-C-5-4-6-1−C2-1-C-5-4-6-5. Separation of C2-1-C-5-4-6-5 (16 mg) by reversed phase HPLC using the same column and the mobile phase of 20% CH_3OH in H_2O containing 0.5% TFA (flow rate 2 mL/min) obtained **3** (5.1 mg, t_R = 44 min).

4.3.1. Aconicarmisulfonine B (*1*)

White amorphous powder (MeOH); $[\alpha]_D^{20}$ −38.1 (*c* 0.29, CH_3OH); UV (CH_3OH) λ_{max} (logε) 202 (2.24), 223 (sh, 1.62), 267 (0.89) nm; CD (CH_3OH) λ_{max} ($\Delta\varepsilon$) 200 (−1.18), 290 (−0.43), 329 (+0.04); IR ν_{max} 3393, 2970, 2922, 2850, 1738, 1678, 1485, 1466, 1420, 1321, 1202, 1140, 1049, 957, 905, 879, 838, 801, 722 cm^{-1}; ^1H NMR (D_2O, 600 MHz) spectroscopic data, see Table 1; ^{13}C NMR (D_2O, 150 MHz) spectroscopic data (Table 1); ^1H NMR (CD_3OD, 600 MHz) spectroscopic data (Table S1); ^{13}C NMR (CD_3OD, 150 MHz) spectroscopic data (Table S1); (+)-ESI-MS *m/z* 438 $[M+H]^+$, 460 $[M+Na]^+$, (−)-ESI-MS *m/z* 436 $[M-H]^-$; (+)-HR-ESI-MS *m/z* 438.1954 $[M+H]^+$ (Calcd. for $C_{22}H_{32}NO_6S$, 438.1945), (−)-HR-ESI-MS *m/z* 436.1813 $[M-H]^-$ (Calcd. for $C_{22}H_{30}NO_6S$, 436.1799).

4.3.2. Aconicarmisulfonine C (*2*)

White amorphous powder (CH_3OH); $[\alpha]_D^{20}$ −37.4 (*c* 0.14, CH_3OH); UV (CH_3OH) λ_{max} (logε) 202 (2.46), 219 (sh, 1.65) nm; CD (CH_3OH) λ_{max} ($\Delta\varepsilon$) 200 (−0.54), 296 (−0.65); IR ν_{max} 3394, 2920, 2850, 1736 (sh), 1680, 1543, 1448, 1358, 1203, 1140, 1053, 983, 956, 907, 880, 842, 802, 724 cm^{-1}; ^1H NMR (D_2O, 600 MHz) spectroscopic data, see Table 1; ^{13}C NMR (D_2O, 150 MHz) spectroscopic data (Table 1); ^1H NMR (CD_3OD, 600 MHz) spectroscopic data (Table S1); ^{13}C NMR (CD_3OD, 150 MHz) spectroscopic data (Table S1); (+)-ESI-MS *m/z* 438 $[M+H]^+$, 460 $[M+Na]^+$, 476 $[M+K]^+$, (−)-ESI-MS *m/z* 436 $[M-H]^-$; (+)-HR-ESI-MS *m/z* 438.1945 $[M+H]^+$ (Calcd. for $C_{22}H_{32}NO_6S$, 438.1945), (−)-HR-ESI-MS *m/z* 436.1813 $[M-H]^-$ (Calcd. for $C_{22}H_{30}NO_6S$, 436.1799).

4.3.3. Chuanfusulfonine A (*3*)

White amorphous powder (CH_3OH); $[\alpha]_D^{20}$ −7.3 (*c* 0.15, CH_3OH); UV (CH_3OH) λ_{max} (logε) 202 (2.48), 222 (sh, 1.48) nm; CD (CH_3OH) λ_{max} ($\Delta\varepsilon$) 220 (+0.05), 250 (−0.04), 296 (−0.09); IR

Table 2 Experimental data for the analgesic effect of compounds **1**−**3**, **4a**, **4c, 5**, **5a**, and **5b**.

Group	Reagent	Dose (mg/kg)	Number of mice	Number of writhing	Percent inhibition (%)
Vehicle group	Normal saline	0.0	10	36.22 ± 2.50	0.0
Positive group	Flaconitine	0.3	10	10.4 ± 2.62***	71.28
Test group	**1**	1.0	10	24.9 ± 4.61*	31.26
		0.3	10	35.3 ± 1.60	2.55
		0.1	10	34.9 ± 2.41	3.65
	2	1.0	10	26.5 ± 3.53*	26.84
		0.3	10	35.5 ± 1.69	1.99
		0.1	10	31.8 ± 4.13	12.20
	3	1.0	10	32.9 ± 4.35	9.17
		0.3	10	33.1 ± 4.42	8.62
		0.1	10	34.1 ± 4.56	5.85
	4a	1.0	10	29.9 ± 4.21	17.45
		0.3	10	30.1 ± 4.03	16.07
		0.1	10	38.2 ± 3.17	0.0
	4c	1.0	10	31.4 ± 6.66	13.31
		0.3	10	30.9 ± 4.13	14.69
		0.1	10	35.8 ± 5.94	1.16
	5	1.0	10	17.7 ± 2.45***	51.13
		0.3	10	25.9 ± 2.98*	28.49
		0.1	10	35.6 ± 2.32	1.72
	5a	1.0	10	18.5 ± 2.29**	48.92
		0.3	10	26.2 ± 4.61	27.66
		0.1	10	30.3 ± 4.82	16.35
	5b	1.0	10	23.8 ± 3.10*	34.29
		0.3	10	25.6 ± 3.11	29.32
		0.1	10	36.5 ± 3.64	0.0

Note: data are expressed as mean ± SEM, $*P < 0.05$, $**P < 0.01$, $***P < 0.001$ compared to the model group.

ν_{max} 3395, 3185, 3011, 2922, 2849, 1731, 1646, 1539, 1468, 1419, 1343, 1324, 1301, 1214, 1188, 1119, 1026, 802, 722, 647 cm^{-1}; ^1H NMR (D_2O, 600 MHz) spectroscopic data (Table 1); ^{13}C NMR (D_2O, 150 MHz) spectroscopic data (Table 1); (+)-ESI-MS *m/z* 456 $[M+H]^+$, 478 $[M+Na]^+$, 494 $[M+K]^+$, (−)-ESI-MS *m/z* 454 $[M-H]^-$; (+)-HR-ESI-MS *m/z* 478.1882 (Calcd. for $C_{22}H_{33}NO_7SNa$, 478.1870), (−)-HR-ESI-MS *m/z* 454.1916 $[M-H]^-$ (Calcd. for $C_{22}H_{32}NO_7S$, 454.1905).

4.3.4. *ECD calculations of **1**−**3***

See Supporting Information.

4.3.5. *Isolation and structural characterization of **1-d**, **2-d**, **4a**, **4b**, and **4c***

The samples of **1** (3.0 mg) and **2** (1.8 mg) in D_2O, which were stored in a refrigerator at 4 °C for 14 months and detected by the NMR spectral measurements to be identical, were combined and evaporated under reduced pressure to give a mixture. The mixture was separated by HPLC using the YMC-Pack Ph column and the mobile phase of 20% CH_3OH in H_2O containing 0.5% TFA (flow rate 2 mL/min) to afford two compounds. The ^1H NMR spectrum of the major compound (3.8 mg, t_R = 37 min) in D_2O indicated it was **1-*d***. However, the ^1H NMR spectrum of the minor one (0.4 mg, t_R = 31 min) in D_2O was almost identical to that of the mixture prior to HPLC separation. Because the two peaks in the HPLC chromatogram were completely separated, the minor compound must be **2-*d*** and was partially transformed again into **1-*d*** during evaporation of the HPLC mobile phase. Although further isolation of **2-*d*** failed due to limitation of the sample amount, the structure was able to be determined by 2D NMR spectroscopic data analysis of the mixtures acquired prior to HPLC separation, while the ^1H and ^{13}C NMR (D_2O or CD_3OD, 600 MHz) spectroscopic data of **1-*d*** and **2-*d*** (Tables S1 and S2) were unambiguously assigned.

The sample of **4** (4.2 mg) in D_2O with sodium 3-trimethylsilylpropionate (TMSP-2,2,3,3-d_4), which showed gradual production of **4a** by the NMR spectra as an internal reference, was evaporated under reduced pressure to give a residue. Isolation of the residue by HPLC (YMC-Pack Ph column, 15% CH_3OH in H_2O containing 0.1% TFA, flow rate 2 mL/min) yield **4a** (0.8 mg, t_R = 28 min) and **4** (3.1 mg, t_R = 31 min). Recovery of **4** was proved by complete identity of the ^1H NMR spectrum with that of the original sample. **4a**: white amorphous powder; ^1H NMR (D_2O, 600 MHz) spectrpscopic data (Table S3); ^{13}C NMR (D_2O, 150 MHz) spectroscopic data (Table S3); (+)-HR-ESI-MS *m/z* 436.17902 $[M+H]^+$ (Calcd. for $C_{22}H_{30}NO_6S$, 436.17883), (−)-HR-ESI-MS *m/z* 434.16486 $[M-H]^-$ (Calcd. for $C_{22}H_{28}NO_6S$, 434.16428).

The sample of **4** (4.0 mg) in pyridine-d_5, of which the NMR spectra showed gradual generation of **4b**, was further carried out the 2D NMR experiments. The structure of **4b** was determined by analysis of the 2D NMR spectroscopic data, for which the ^1H NMR (D_2O, 600 MHz) and ^{13}C NMR (D_2O, 150 MHz) spectroscopic data were assigned (Table S3). Then the sample was evaporated under reduced pressure to give a mixture. HPLC separation of the mixture (YMC-Pack Ph column, 15% CH_3OH in H_2O containing 0.1% TFA, flow rate 2 mL/min) yielded **4c** (1.0 mg, t_R = 18 min) and **4** (2.9 mg, t_R = 31 min). **4c**: white amorphous powder; ^1H NMR (D_2O, 600 MHz) spectrpscopic data (Table S3); ^{13}C NMR (D_2O, 150 MHz) spectroscopic data (Table S3); (+)-HR-ESI-MS *m/z* 434.16345 $[M+H]^+$ (Calcd. for

$C_{22}H_{28}NO_6S$, 434.16318), (−)-HR-ESI-MS *m/z* 432.14917 $[M-H]^-$ (Calcd. for $C_{22}H_{26}NO_6S$, 432.14863).

4.3.6. *Reaction of* ***5*** *with sodium bisulfite*

Compound **5** (10.2 mg) and sodium bisulfite (Na_2SO_3, 20.0 mg) were dissolved in CH_3OH/H_2O (1:1, 10.0 mL) and kept at room temperature for 24 h. With TLC detection, no product was formed in the reaction mixture. Then the solution was refluxed for 8 h and two compounds were produced as detected by TLC. After remove of the solvent, the residue was separated by HPLC (YMC-Pack Ph column, 25% CH_3OH in H_2O containing 0.1% TFA, flow rate 2 mL/min) to yield **5a** (1.6 mg, t_R = 26 min) and **5b** (3.8 mg, t_R = 28 min). **5a**: white amorphous powder; ^1H NMR (D_2O, 600 MHz) spectrpscopic data (Table S4); ^{13}C NMR (D_2O, 150 MHz) spectroscopic data (Table S4); (−)-HR-ESI-MS *m/z* 330.2070 $[M-H]^-$ (Calcd. for $C_{20}H_{28}NO_3$, 330.2064). The spectroscopic data **5b** were completely indental with the reported data of aconicarmichinium B[42].

4.5. *Acetic acid-induced writhing test*

See Supporting Information.

Acknowledgments

Financial support of the National Natural Sciences Foundation of China (81630094, 21732008, and 81730093), CAMS Innovation Fund for Medical Science of China (2017-I2M-3-010 and 2016-I2M-1-010), and the Drug Innovation Major Project (2018ZX09711001-001-001, 2018ZX09711001-001-003, and 2018ZX09711001-003-001, China) is acknowledged.

Author contributions

Jiangong Shi designed and guided all the chemical experiments, analyzed the data, and rewrote and revised the manuscript. Qinglan Guo and Huan Xia conducted the chemical experiments, doublechecked the data, and wrote the preliminary manuscript. Tiantai Zhang designed the pharmacological test and analyzed the corresponding data. Shuai Shao conducted the pharmacological experiments. Yuzhuo Wu and Chengbo Xu assisted the chemical experiments. All authors read and approved the final manuscript.

Conflicts of interest

The authors have no conflicts of interest to declare.

Appendix A. Supporting information

Supporting data to this article can be found online at https://doi.org/10.1016/j.apsb.2020.01.013.

References

1. Wang FP, Liang XT. The C_{20}-diterpenoid alkaloids. In: Cordell GA, editor. *The alkaloids: chemistry and biology*, vol. 59. New York: Elsevier Science; 2002. p. 1−280.
2. Wang FP, Chen QH, Liu XY. Diterpene alkaloids. *Nat Prod Rep* 2010;**27**:529−70.
3. Zhang ZT, Liu XY, Chen DL, Wang FP. New diterpenoid alkaloids from *Aconitum liangshanicum*. *Helv Chim Acta* 2010;**93**:811−7.
4. Tang H, Wen FL, Wang S-H, Liu XY, Chen DL, Wang FP. New C_{20}-diterpenoid alkaloids from *Aconitum sinomontanum*. *Chin Chem Lett* 2016;**27**:761−3.
5. Tang TX, Chen QF, Liu XY, Jian XX, Wang FP. New C_{20}-diterpenoid alkaloids from *Aconitum vilmorrianum* and structural revision of 2-*O*-acetylorochrine and orochrine. *J Asian Nat Prod Res* 2016;**18**:315−27.
6. Wang FP, Liang XT. Chemistry and pharmacology. In: Cordell GA, editor. *The alkaloids*, vol. 42. New York: Academic Press; 1992. p. 151−248.
7. Liu XY, Qin Y. Enabling syntheses of diterpenoid alkaloids and related diterpenes by an oxidative dearomatization/Diels−Alder cycloaddition strategy. *Nat Prod Rep* 2017;**34**:1044−50.
8. Kou KGM, Pflueger JJ, Kiho T, Morrill LC, Fisher EL, Clagg K, et al. A benzyne insertion approach to hetisine-type diterpenoid alkaloids: synthesis of cossonidine (davisine). *J Am Chem Soc* 2018;**140**:8105−9.
9. Zhou S, Guo R, Yang P, Li A. Total synthesis of septedine and 7-deoxyseptedine. *J Am Chem Soc* 2018;**140**:9025−9.
10. Zhang QZ, Zhang ZS, Huang Z, Zhang CH, Xi S, Zhang M. Stereoselective total synthesis of hetisine-type C_{20}-diterpenoid alkaloids: spirasine IV and XI. *Angew Chem Int Ed* 2018;**57**:937−41.
11. Liu J, Ma D. A unified approach for the assembly of atisine- and hetidine-type diterpenoid alkaloids: tyotal syntheses of azitine and the proposed structure of navirine C. *Angew Chem Int Ed* 2018;**57**:6676−80.
12. Nie W, Gong J, Chen Z, Liu J, Tian D, Song H, et al. Enantioselective total synthesis of (−)-arcutinine. *J Am Chem Soc* 2019;**141**:9712−8.
13. Jiangsu New Medical College. *Dictionary of traditional Chinese medicine*, vol. 1. Shanghai: Shanghai Science and Technology Publishing House; 1995. p. 228−32, 1191−4.
14. Konno C, Shirasaka M, Hikino H. Structure of senbusine A, B and C, diterpenic alkaloids of *Aconitum carmichaeli* roots from China. *J Nat Prod* 1982;**45**:128−33.
15. Shim SH, Lee SY, Kim JS, Son KH, Kang SS. Norditerpenoid alkaloid and other components from the processed tubers of *Aconitum carmichaeli*. *Arch Pharm Res* 2005;**28**:1239−43.
16. Chang YT, Wu JY, Liu TP. On the toxicity of Fu-Tze (*Aconitum chinense*). *Acta Pharm Sin* 1966;**13**:350−5.
17. Bisset NG. Arrow poisons in China. Part II. *Aconitum*-Botany, chemistry, and pharmacology. *J Ethnopharmacol* 1981;**4**:247−336.
18. Zhou YP. Pharmacological effects and toxicities of fuzi and its main chemical constituents. *Acta Pharm Sin* 1983;**18**:394−400.
19. Chan TYK. Aconite poisoning. *Clin Toxicol* 2009;**47**:279−85.
20. Zhou GH, Tang LY, Zhou XD, Wang T, Kou ZZ, Wang ZJ. A review on phytochemistry and pharmacological activities of the processed lateral root of *Aconitum carmichaelii* Debeaux. *J Ethnopharmacol* 2015;**160**:173−93.
21. Lu G, Dong Z, Wang Q, Qian G, Huang W, Jiang Z, et al. Toxicity assessment of nine types of decoction pieces from the daughter root of *Aconitum carmichaeli* (Fuzi) based on the chemical analysis of their diester diterpenoid alkaloids. *Planta Med* 2010;**76**:825−30.
22. Wen RQ, Li DH, Zhao X, Wang JB, Zhao YL, Zhang P, et al. Rationality of the processing methods of Aconiti Lateralis Radix (Fuzi) based on chemical analysis. *Acta Pharm Sin* 2013;**48**:286−90.
23. Kuang Q, Hou D, Sun H, Yue C. Effect of different decocting time on contents of ester-type alkaloids in water decoction of *Aconitum carmichaeli* Dexb. *Liaoning J Tradit Chin Med* 2014;**41**:1707−9.
24. Liang Y, Wu JL, Li X, Guo MQ, Leung ELH, Zhou H, et al. Anticancer and anti-inflammatory new vakognavine-type alkaloid from the roots of *Aconitum carmichaelii*. *Tetrahedron Lett* 2016;**57**:5881−4.
25. Zong XX, Yan G, Wu JL, Leung ELH, Zhou H, Li N, et al. New C_{19}-diterpenoid alkaloids from the parent roots of *Aconitum carmichaelii*. *Tetrahedron Lett* 2017;**58**:1622−6.
26. Yu J, Yin TP, Wang JP, Mei RF, Cai L, Ding ZT. A new C_{20}-diterpenoid alkaloid from the lateral roots of *Aconitum carmichaelii*. *Nat Prod Res* 2017;**31**:228−32.

27. Qin XD, Yang S, Zhao Y, Gao Y, Ren FC, Zhang DY, et al. A new aporphine alkaloid from *Aconitum carmichaelii*. *Chem Nat Compd* 2017;**53**:501−3.
28. Li Y, Gao F, Zhang JF, Zhou XL. Four new diterpenoid alkaloids from the roots of *Aconitum carmichaelii*. *Chem Biodivers* 2018;**15**:e1800147.
29. Zong XX, Yan X, Wu JL, Liu Z, Zhou H, Li N, et al. Potentially cardiotoxic diterpenoid alkaloids from the roots of *Aconitum carmichaelii*. *J Nat Prod* 2019;**82**:980−9.
30. Do TQ, Truong BN, Mai HDT, Nguyen TL, Nguyen VH, Nguyen HD, et al. New dianthramide and cinnamic ester glucosides from the roots of *Aconitum carmichaelii*. *J Asian Nat Prod Res* 2019;**21**:507−15.
31. Zhou X, Guo QL, Zhu CG, Xu CB, Wang YN, Shi JG. Gastradefurphenol, a minor 9,9′-neolignan with a new carbon skeleton substituted by two *p*-hydroxybenzyls from an aqueous extract of "tian ma". *Chin Chem Lett* 2017;**28**:1185−9.
32. Liu Y, Chen M, Guo Q, Li Y, Jiang J, Shi J. Aromatic compounds from an aqueous extract of "ban lan gen" and their antiviral activities. *Acta Pharm Sin B* 2017;**7**:179−84.
33. Meng L, Guo Q, Liu Y, Chen M, Li Y, Jiang J, et al. Indole alkaloid sulfonic acids from an aqueous extract of *Isatis indigotica* roots and their antiviral activity. *Acta Pharm Sin B* 2017;**7**:334−41.
34. Meng LJ, Guo QL, Xu CB, Zhu CG, Liu YF, Chen MH, et al. Diglycosidic indole alkaloid derivatives from an aqueous extract of *Isatis indigotica* roots. *J Asian Nat Prod Res* 2017;**19**:529−40.
35. Meng L, Guo Q, Liu Y, Shi J. 8,4′-Oxyneolignane glucosides from an aqueous extract of "ban lan gen" (*Isatis indigotica* root) and their absolute configurations. *Acta Pharm Sin B* 2017;**7**:638−46.
36. Meng L, Guo Q, Zhu C, Xu C, Shi J. Isatindigodiphindoside, an alkaloid glycoside with a new diphenylpropylindole skeleton from the root of *Isatis indigotica*. *Chin Chem Lett* 2018;**29**:119−22.
37. Guo Q, Xu C, Chen M, Lin S, Li Y, Zhu C, et al. Sulfur-enriched alkaloids from the root of *Isatis indigotica*. *Acta Pharm Sin B* 2018;**8**:933−43.
38. Meng L, Guo Q, Chen M, Jiang J, Li Y, Shi J. Isatindolignanoside A, a glucosidic indole-lignan conjugate from an aqueous extract of the *Isatis indigotica* roots. *Chin Chem Lett* 2018;**29**:1257−60.
39. Jiang B, Lin S, Zhu CG, Wang S, Wang Y, Chen M, et al. Diterpenoid alkaloids from the lateral root of *Aconitum carmichaelii*. *J Nat Prod* 2012;**75**:1145−59. 1878 and 2008.
40. Jiang ZB, Jiang BY, Zhu CG, Guo QL, Peng Y, Wang XL, et al. Aromatic acid derivatives from the lateral roots of *Aconitum carmichaelii*. *J Asian Nat Prod Res* 2014;**16**:891−900.
41. Jiang ZB, Meng XH, Jiang BY, Zhu CG, Guo QL, Wang SJ, et al. Two 2-(quinonylcarboxamino)benzoates from the lateral roots of *Aconitum carmichaelii*. *Chin Chem Lett* 2015;**26**:653−6.
42. Meng XH, Jiang ZB, Zhu CG, Guo QL, Xu CB, Shi JG. Napelline-type C_{20}-diterpenoid alkaloid iminiums from an aqueous extract of "fu zi": solvent-/base-/acid-dependent transformation and equilibration between alcohol iminium and aza acetal forms. *Chin Chem Lett* 2016;**27**:993−1003.
43. Meng XH, Jiang ZB, Guo QL, Shi JG. A minor arcutine-type C_{20}-diterpenoid alkaloid iminium constituent of "fu zi". *Chin Chem Lett* 2017;**28**:588−92.
44. Meng XH, Guo QL, Zhu CG, Xu CB, Shi JG. Unprecedented C_{19}-diterpenoid alkaloid glycosides from an aqueous extract of "fu zi": neoline 14-*O*-L-arabinosides with four isomeric L-arabinosyls. *Chin Chem Lett* 2017;**28**:1705−10.
45. Guo QL, Xia H, Shi G, Zhang T, Shi JG. Aconicarmisulfonine A, a sulfonated C20-diterpenoid alkaloid from the lateral roots of Aconitum carmichaelii. *Org Lett* 2018;**20**:816−9.
46. Guo Q, Xia H, Meng X, Shi G, Xu C, Zhu C, et al. C_{19}-Diterpenoid alkaloidarabinosides from an aqueous extract of the lateral root of *Aconitum carmichaelii* and their analgesic activities. *Acta Pharm Sin B* 2018;**8**:409−19.
47. Wu Y, Shao S, Guo Q, Xu C, Xia H, Zhang T, et al. Aconicatisulfonines A and B, analgesic zwitterionic C_{20}-diterpenoid alkaloids with a rearranged atisane skeleton from *Aconitum carmichaelii*. *Org Lett* 2019;**21**:6850−4.
48. Lightner DA. The octant rule. In: Nakanishi K, Berova N, Woody RW, editors. *Circular dichroism principles and applications*. New York: Wiley-VCH; 1994. p. 259−300.
49. Ye XL. *Stereochemistry*. Beijing: Beijing University Express; 1999. p. 236−58.
50. Wei XY, Chen SY, Zhou J. Chuanfunine−a new water-soluble diterpenoid alkaloid from *Aconitum carmichaelii* Debx. *Chin J Bot* 1990;**2**:57−63.
51. Sultankhodzhaev MN, Tashkhodzhaev B, Turgunov KK, Kurbanov U Kh, Mukarramov NI. Structure and conformational analysis of napelline-type diterpenoid alkaloids. *Chem Nat Compd* 2017;**53**:99−104.
52. Song ZL, Fan CA, Tu YQ. Semipinacol rearrangement in natural product synthesis. *Chem Rev* 2011;**111**:7523−56.
53. Chen Q. *Experimental methodology of pharmacology*. Beijing: People's Health Press; 2010. p. 742−70.